Journal of Food Research; Vol. 12, No. 2; 2023
ISSN 1927-0887 E-ISSN 1927-0895
Published by Canadian Center of Science and Education

Monitoring Postharvest Color Changes and Damage Progression of Cucumbers Using Machine Vision

Ayesha Sarker[1, 2] & Tony E. Grift[1]

[1] Department of Agricultural and Biological Engineering, University of Illinois Urbana-Champaign, 1304 West Pennsylvania Avenue, Urbana, IL 61801, USA

[2] Agricultural and Environmental Research Station, West Virginia State University, Institute, WV 25112, USA

Correspondence: Ayesha Sarker, Agricultural and Environmental Research Station, West Virginia State University, Institute, WV 25112, USA. E-mail: ayesha.sarker@wvstateu.edu
ORCHID ID: https://orcid.org/0000-0002-4458-308X

Received: February 8, 2023 Accepted: April 12, 2023 Online Published: April 18, 2023

doi:10.5539/jfr.v12n2p37 URL: https://doi.org/10.5539/jfr.v12n2p37

Abstract

To monitor cucumbers' external quality, such as color changes or the presence of any damage during storage, a machine vision system was used. Red, Green, Blue (RGB) images were acquired in a "soft box," which provided a highly diffused lighting scene for observing visual changes such as color and appearance in the skin of cucumber. The RGB images were transformed into L*, a*,b*, and HSV spaces. Histograms for each channel in each color space were evaluated for image segmentation, and the blue (B) channel in the RGB color space was found superior in terms of measuring damage progression. Damage progression plots (DPP) were made from accumulated grayscale images in each of the color channels and to observe variation over time, absolute differential damage progression (ADDP) plots were generated. Overall, the order of channel utility was [B], [R, G, V], and [H, S, L*, a*, b*]. To assess which channel, in which colorspace, was most sensitive, i.e., could capture most of the information regarding day-to-day color changes, a principal component analysis (PCA) was performed. The PCA showed that all individual components in the RGB color space were suitable for obtaining information about the external changes of cucumber. Based on the results, the machine vision approach is recommended as a non-destructive technique for monitoring the external quality of stored fresh produce.

Keywords: postharvest, machine vision, color spaces, color change, defects, image processing, 3-D histogram

Highlights:

1. A machine vision system was used for non-destructive quality evaluation of cucumbers.
2. From images, changes in R, G, and B values indicated the corresponding color changes.
3. Blue (B) channel in RGB color space best interpreted the damage progression.
4. RGB was found to be the most suitable color space based on PCA.

List of Abbreviations

ADDP	: Absolute differential damage progression
CCPA	: Cucumber center pixel accumulation algorithm
DPP	: Damage progression plot
HDPE	: High-density polyethylene
HSV	: Hue, Saturation, Value
PCA	: Principal component analysis
RGB	: Red, Green, Blue

1. Introduction

The quality of cucumbers may deteriorate both externally and internally during harvesting, transport, and postharvest handling (Mohammadi et al., 2016). Damage or decay on the cucumber surface results in rejection by consumers, causing economic loss to producers (Ariana and Lu, 2010). At harvest time, the cucumber skin color should be a uniform dark green; fruits with yellow skin and tough seeds are deemed as overmature and of

low quality (New Guyana Marketing Corporation, n.d.). Additional quality indices are a uniform shape and absence of defects from handling or decay from fungal and bacterial diseases.

Destructive and nondestructive - these are the two ways quality attributes can be measured. Non-destructive approaches offer rapid measurement, which reduces waste and maintains the appearance of the fruit (Nicolaï et al., 2014). In addition, repetitive measurements of quality parameters of the same fruits throughout an experiment are feasible in a non-destructive technique (Iqbal et al., 2016). Non-destructive machine vision-based quality monitoring techniques have been largely applied in postharvest sectors (Kondo, 2010). Machine vision technology is being used for automatic grading and quality inspection of fresh commodities, especially fruits and vegetables (Cubero et al., 2011; Mohammadi et al., 2015). The computer vision system has been replacing human inspection (Du and Sun, 2006) because manual performance is affected by fatigue, may involve large errors, and be cost-prohibitive (Ariana & Lu, 2010; Iqbal et al., 2016). Machine vision has been used either to inspect products' quality parameters such as maturity, color, size, defects, etc., for grading purposes or to monitor a product's evolution as a function of time to evaluate a treatment or a process (Cubero et al., 2011; Akundi & Reyna, 2021).

Color is one of the critical quality parameters that indicates the quality, maturity, and senescence of fruits and vegetables (Mendoza et al., 2006; Mohammadi et al., 2015). In fact, consumers accept or reject a fruit or vegetable primarily based on color (Cubero et al., 2011; Sarker et al., 2021). Colorimeters are generally used to measure color, but they are not well suited to measure the color of a large area or of objects with non-uniform color characteristics (Gardner, 2007). Therefore, a still or video camera can be employed to image a large area with or without heterogeneous color where the colors can be discriminated by the pixels. RGB (red, green, and blue) space is the most widely used color space in computers and digital images to express the color of a pixel (Cubero et al., 2011). Other color spaces that are frequently used are L* a* b* and Hue, Saturation and Value (HSV) (Bhargava & Bansal, 2021). RGB color space values can be easily converted to HSV and L* a* b* following image processing algorithms to quantify the color of products (Mendoza et al., 2006; Fathi et al., 2009; Momin et al., 2017).

The objectives of this study were: (i) to design and implement a computer vision system for continuous monitoring of cucumber external quality, such as color and damage progression over time (ii) to compare the suitability of RGB, L* a* b* and HSV color spaces in terms of their sensitivity to color changes and damage progression in stored cucumber.

2. Materials and Methods

To acquire images from various cucumbers, an imaging arrangement used in earlier research where corn roots (Grift et al., 2011) and ears were studied (Grift et al., 2017) was adapted. In addition, acquisition and analysis software that was used in earlier research was repurposed using Matlab's Appdesigner tool.

2.1 Imaging Arrangement

Cucumber images were acquired in a "soft box," (Grift et al., 2011; Grift et al., 2017) as shown in Fig. 1a. The soft box was made of HDPE panels, creating a highly diffuse lighting scene with low glare (halation) on the cucumber, which is important to obtain true color information from cucumbers. While acquiring images, a cucumber was placed on a 6.35 mm spike that was rotated by a uni-polar 12 V DC 600 mA stepper motor (part no. 162027, Jameco, Belmont, CA). The stepper motor has a stepping angle of $0.9°$ in half step mode, allowing up to 400 unique images per revolution. An aluminum coupler connected the mounting spike to the stepper motor. The adjustable coupler also helped the cucumber reach the height necessary for imaging the quasi-cylindrical mid-section (qcms) of the cucumber. The stepper motor was controlled by a board with a serial interface (model STP100, Pontech, Rancho Cucamonga, CA) and a 12 V, 60 W power supply (part no. 2105308, Jameco, Belmont, CA). The bottom part of the cucumber was contained within a 3D printed tri-pod holder to prevent cucumber slippage during rotation. Fig. 1a shows a photo of the imaging arrangement; a lateral color camera (Unibrain, model 701c) with a resolution of 1280*960 pixels was mounted in the side panel of the soft box.

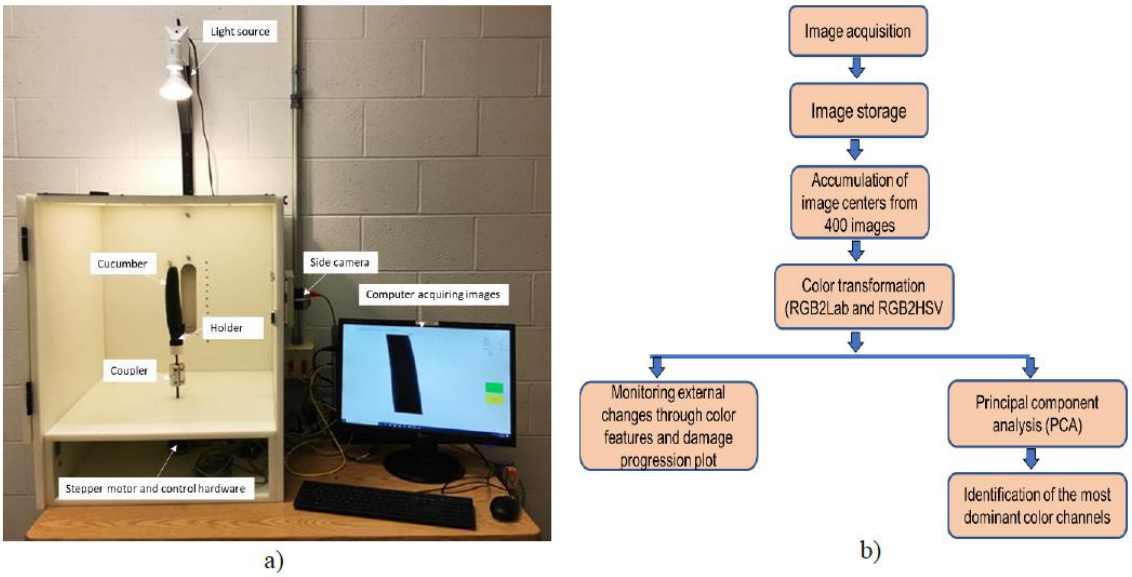

Figure 1. Cucumber imaging arrangement (a) and schematic diagram of assessing postharvest quality of cucumbers (b)

2.2 Cucumber Imaging

The camera and the imaging process in general were controlled by an app written in the Appdesigner tool (MatLab , R2020a). The user can set the serial communication port controlling the stepper motor driver board for cucumber rotation, the delay time for the cucumber to come to rest after being rotated, as well as the sample barcode. The light intensity in the imaging box was calibrated with the cucumber placed inside. During calibration, the app gradually increased the shutter time of the camera until it reaches an image intensity at which all image corner pixels achieve a value of 255 (white).

The lateral camera takes images of the quasi-cylindrical mid-section (Grift et al., 2017), which is approximately 10 cm in height. To take 400 images (represented by 400 pulses to the stepper motor) in one revolution that is equal to 360 °, the cucumber rotates at an angle of 0.9 ° per step. To monitor the cucumber's physical change, continuous imaging was carried out up to one week. The schematic of the whole study is shown in Fig. 1b. For 'weekly' imaging, 400 images were captured at each whole hour throughout the week, resulting in 67,200 (400*24*7) images.

2.3 Cucumber Center Pixel Accumulation (CCPA) Algorithm

To evaluate the damage that a cucumber accumulated during storage, an image is required that covers the cucumber’s quasi-cylindrical mid-section (qcms) surface without redundancy. This overall image should ideally be rectangular for easy manipulation in software. Shown in Fig. 2a is a cucumber at the end of a one-week long study, after it was exposed to high temperatures. This cucumber is obviously severely damaged, being on the verge of collapse. To acquire rectangular images representing the qcms surface without redundancy, a Cucumber Center Pixel Accumulation (CCPA) algorithm was developed. The CCPA algorithm collected a vector of pixels from the center (“spine”) of each image of the qcms with a size of 1*1280 pixels. This was done by first converting the RGB image into a grayscale image, as shown in Fig. 2a, right, and then by finding the edges of the cucumber for each row. The selected Center pixel was chosen at the location of the mean of the edge pixels, as shown as the plotted line in the right hand image of Fig. 2a.

a) b)

Figure 2. Shown is an image of a cucumber that is severely damaged (a) and Center Pixel Accumulation image with a size of 1280*400 pixels (b)

The center pixels selection process was repeated from the top (row 1) to the bottom (row 1280), yielding a Center Pixel vector of 1280*1 pixels per image. This process was repeated 400 times on images that are rotated by 0.9 ° each, and the center pixel vectors were accumulated, forming a 1280*400-pixel sized image that covers the complete qcms without redundancy. Figure 2b shows the Center Pixel Accumulation image from the cucumber, as shown in Fig. 2a. This image was used to determine the damage progression of the cucumber.

2.4 Histograms from RGB Images

In this experiment, the whole cucumber surface captured by combining strip centers of 400 RGB images (400 pixels) were examined to interpret color changes. Color histograms of the images were computed by MATLAB R2020a (The MathWorks, Inc., Natick, MA, USA) imhist () function; imhist () computes the histogram of the grayscale image by converting RGB values to grayscale values with a weighted sum of the *R*, *G*, and *B* components according to Eqn. 1:

$$0.2989 * R + 0.5870 * G + 0.1140 * B \quad (1)$$

2.5 Damage Progression Plot (DPP)

To observe the progression of damage, incremental images on a grayscale were plotted by taking images from a certain hour step. For example, to obtain 9 (arbitrary choice) accumulated images, images at 14 hours step up to 140 hours were considered (1:14:140). For easy manipulation of the input parameters, an analysis app was developed using the Appdesigner tool in MatLab (R2020a). To detect changes over time, three plots were made for a range of nine color space channels being R, G, B, H, S, V, L*, a*, b*. First is the damage progression plot (DPP), which comprises accumulated raw grayscale images for individual channels plotted side by side. From Fig. 3, as the days progressed, the white areas at the top were moving downward because the cucumber changed size and shape as it collapsed. Finally, an absolute differential damage progression (ADDP) plot was made, where the first image was subtracted from all other images. The assumption here was that the first image was damage free, and therefore any change in greyscale should be assumed damage. In the ADDP plot, any one channel (for example, either R, G, or B) from the RGB, L*a*b* or HSV color space was considered and subtracted the previous image from the current one.

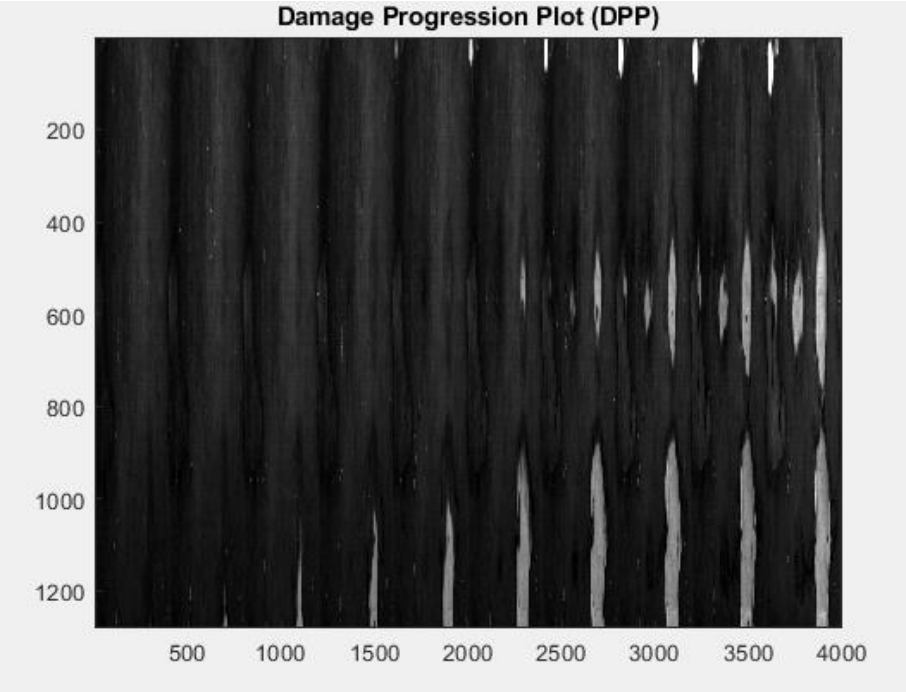

Figure 3. Grayscale Damage Progression Plot (DPP) to visualize the damages that happened over time

2.6 Principal Component Analysis (PCA)

Principal component analysis (PCA) is a statistical tool that gives the direction where the data have the maximal amount of variance. PCA has been used to reduce the dimensionality in a dataset and, therefore, helps in data interpretation (Chherawala et al., 2006). In this work, PCA was performed using prcomp () function of R statistical software (R Core Team, 2019) version 3.5.2. Before performing the analysis, the variables were shifted to be zero centered (center = TRUE) and were scaled to have unit variance (scale. = TRUE) to account for different data set sizes. To clearly visualize the most correlated variables in the dataset, a correlation plot (Fig. 8b) using corrplot () function in R of the variables was made. In the correlation plot (Fig. 8b), positive correlations were indicated by a blue color, and negative correlations were indicated by a red color, and the magnitude of the correlations was displayed by the color intensity and size of the circle.

2.7 Image Processing

Cucumber Center Pixel Accumulation and all the algorithms for color space conversion (RGB2Lab and RGB2HSV), color analysis and visualization, and damage progression plot (DPP) were written in MATLAB R2020b (The MathWorks, Inc., Natick, MA, USA).

3. Results and Discussion

Cucumbers' external changes such as color or appearance of a damage/defects over the storage were described through plotting RGB histograms from the images. In addition, damage progression plots were computed, and the color channels' sensitivity to the damage progression over time was compared. Principal component analysis (PCA) was carried out to find the most dominant component of a color space for its sensitivity to color changes.

3.1 Histogram from RGB Images

Figure 4 shows the images of cucumber on day 1, day 7, day 12, and day 14 and the corresponding color histograms of images. In the histogram of day 1 image, all the pixels were located to the left of the plot and compressed to a small range as demonstrated by larger peaks, which was representative of a fresh dark green cucumber surface. In day 7 histogram, pixels were spread to the center, indicating that the surface was turning into a lighter green color. However, the histogram depicts that there were still dominant darker pixels in the image. Due to the sign of aging and yellowing of cucumber at day 12, the pixels were spread out from the left corner to the right corner in the histogram. On the other hand, from day 14 image, yellowness was prevalent on almost the entire cucumber surface, and in the histogram, the pixels were reached to the extreme right representing a large range of intensities with shorter peaks. Because of this heterogeneous distribution of colors,

unlike colorimeters having a small viewing field, non-destructive machine vision approach capturing the whole surface of a fresh produce could provide a complete data for monitoring any defects and color changes during storage. Further, to understand the changes of R, G, and B components with the increment of storage days, the R, G, and B values were examined and the mean data are shown in Table 2; it was observed that there was a steady increase in each of the R, G, and B values in general indicating that the surfaces were turning into lighter colors.

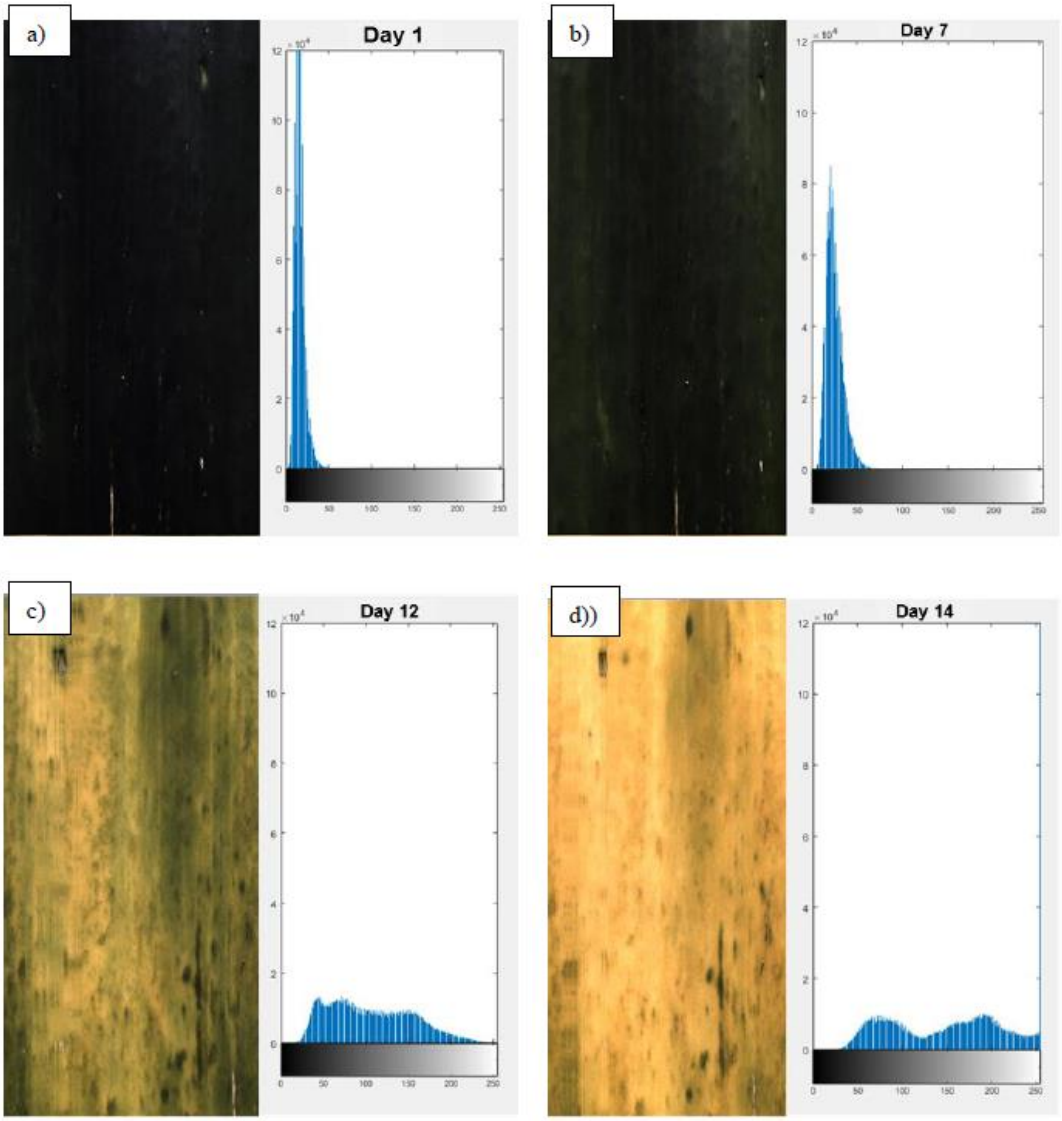

Figure 4. Cucumber image at day 1(a), day 7(b), day 12(c), and day 14(d) with the corresponding RGB histogram at the right (see section 2.4.)

Table 1. Mean R, G, and B values of the RGB images acquired on different days

Sampling days	R	G	B
Day 1	14.738 ±0.55	14.761 ±0.80	14.587 ±1.00
Day 3	16.018 ±0.35	15.896 ±0.41	14.882 ±0.42
Day 5	17.484 ±0.70	17.886 ±0.87	15.647 ±0.90
Day 7	23.093 ±1.60	24.972 ±2.00	18.239 ±1.03
Day 9	40.696 ±4.00	43.038 ±4.20	25.361 ±1.92
Day 12	119.841 ±11.05	107.677 ±7.25	49.646 ±3.00
Day 14	203.806 ±11.70	156.506 ±6.78	71.202 ±4.00

Data are represented as Mean ± SD (n=24)

After harvest, water loss, shriveling, yellowing, and fungal decay lead to the rapid quality loss of cucumber. Therefore, cucumber has a shelf-life shorter than 14 days (Bahnasawy and Khater, 2014; Maleki et al., 2018). Color is one of the critical quality parameters which primarily determines consumer acceptability (Mendoza et al., 2006; Cubero et al., 2011). RGB components determining the color and color distribution data from histograms can be used for grading purposes or harvest quality measurements (Kang et al., 2008). Comparing the color histograms and the R, G, and B components of the images of whole cucumbers subjected to different treatments could be a potential non-destructive method to evaluate the performance of any postharvest treatment such as coating, packaging, etc. in terms of reducing the color changes during storage.

3.2 Damage Progression Plot

Figure 5a shows the absolute differential damage progression (ADDP) plot. In the original image on day 1, it was assumed that there was no damage, but it progressed over time up to the last image. To determine the damage from the ADDP plot (Fig. 5a), the image was segmented from the background by a cutoff point 100 (threshold) on the grayscale (100/255), shown in Fig. 5b.

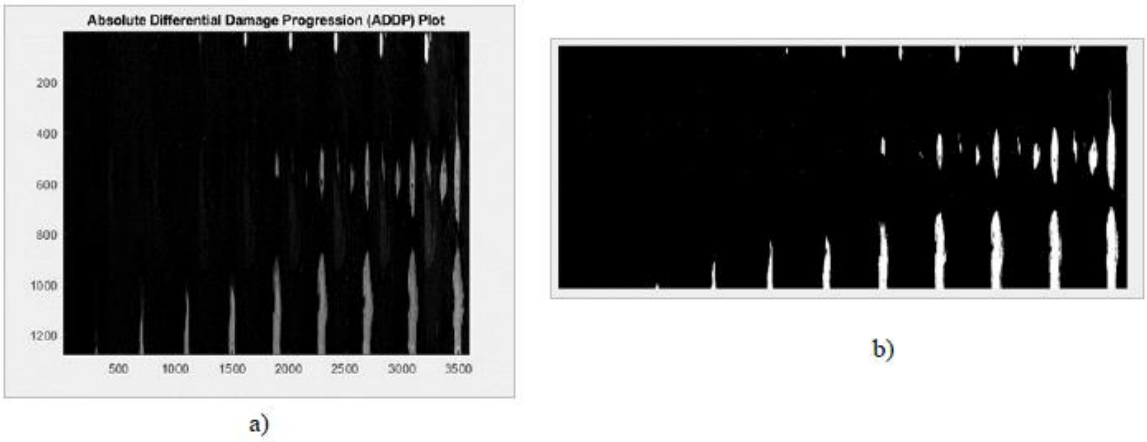

Figure 5. a) Cucumber absolute damage progression plot made with accumulated images in blue (B) color channel, b) Damages that progressed over time were segmented from the background in the absolute damage progression plot

To identify the color channel among R,G,B, L*, a*, b*, H,S,V that gave the most interpretable information on the damage progression, combined histograms of 9 images from each of the ADDP plots were made and compared. Fig. 6 shows the 9 histograms of each ADDP image made in each of the color channels of RGB, L*a*b* and HSV. Figure 6c shows 9 histograms in the B channel where the histogram of the first image is in the background and histograms of subsequent images are presented in the front. In the blue (B) channel in RGB color space, there were apparent differences between the background (pixel values < 100) and foreground (pixel values > 100), which offered easy segmentation, and the pixels from the background and the damages that progressed over time have distinct peaks and valleys. On the otherhand, the histograms from the R (Fig. 6a) and G (Fig. 6b) channel had no distinct peaks compared to the B channel (Fig. 6c), therefore indentifying damage from the image through segmentation would be impossible. None of the L*a*b* color channels (Fig. 6d-f), gave information about the damage progression. In the L* (Fig. 6d) and b* (Fig. 6f), there was no useful information because here, the ADDP plots were black. The V channel (Fig. 6i) in the HSV color space worked similar to R and G from the RGB color space. Therefore, the order of channel utility was [B], [R, G, V], and [H, S, L*, a*, b*].

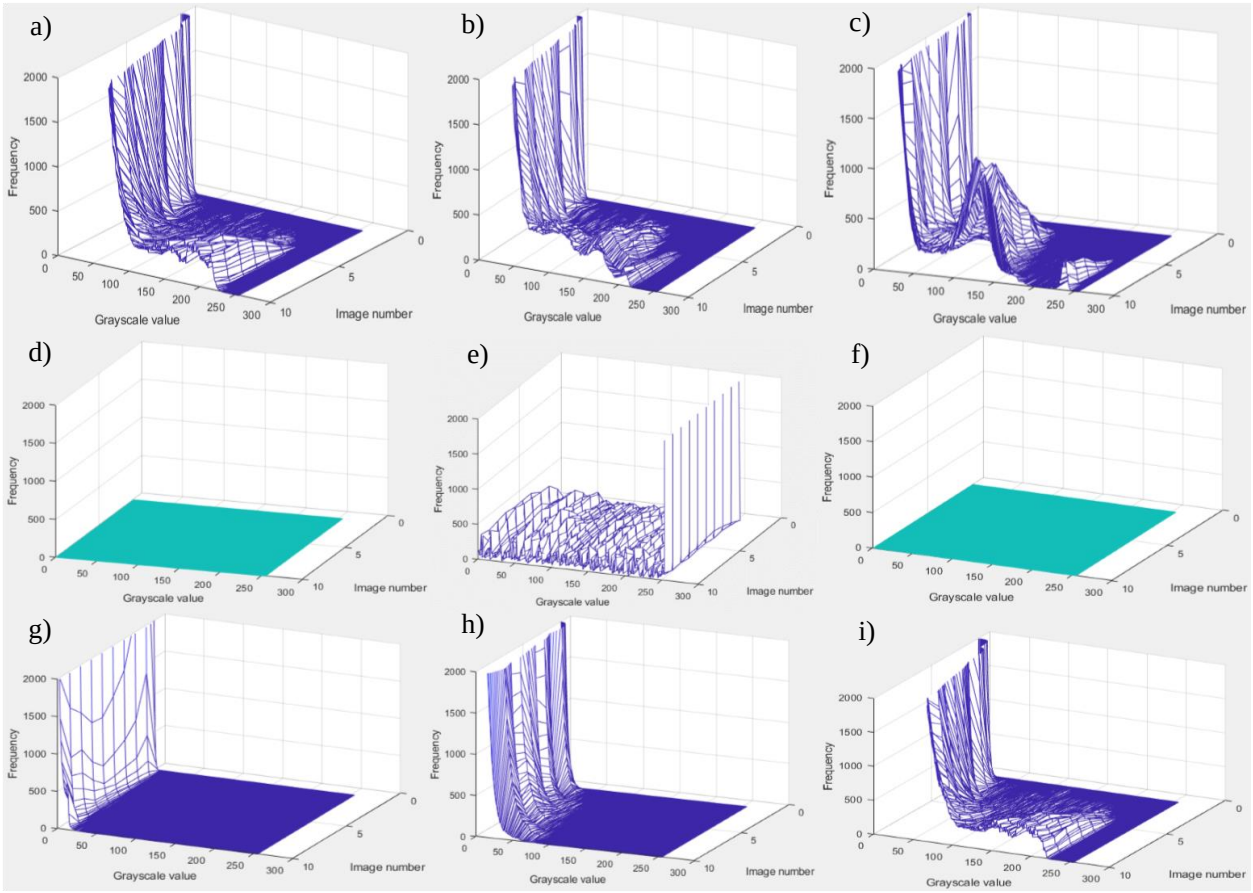

Figure 6. 3-D Histograms of the absolute differential damage progression (ADDP) plot made in different color channels. Top row represents R (a), G (b) and B (c), middle row represents L* (d), a* (e) and b* (f), and bottom row represents H (g), S (h) and V (i). Note: d and f have no information on the histograms because the ADDP plots for L and b color channels were completely black

For further verification, the color channels from all the three-color spaces were compared (Fig. 7). The B channel has clearly segmentable damaged and non-damaged parts (Fig. 7a). In the R and G channel, there were overlaps between the damaged and non-damaged parts (Fig. 7a). In the L*a*b* color space, there was no information on the lightness (L*), the damages, and the background were completely intermingled in the green-red (a*) channel, and little information was obtainable from the blue-yellow channel (b*) (Fig. 7b). On the other hand, in the HSV color space, the Hue (H) channel was completely black (Fig. 7c). The saturation (S) channel had a different color contrast compared to the other channels; it had a gray background and a black foreground that made it difficult to compare with other channels (Fig. 7c). The value (V) appeared similar (Fig. 7c) to the R and G channels.

Similar to present study, disease or damage extensions were reported by color information alone. Damaged surface on dates was identified by image analysis where R from RGB space and H and V from HSV space were used (Al-Rahbi et al., 2013). Maturity stages of persimmon were classified by taking color as an indicator of maturity; R and G from the RGB color space, b* from the L*a*b* color space, and S from the HSI color space, and grey levels were used to define fruit maturity stages (Mohammadi et al., 2015). However, in the present study, to investigate the absolute damage progression over time in cucumber, the plot and the histogram made in the B channel in RGB color space was optimal. It must be noted that the method applied here was merely tested on a single cucumber with extreme damage. Nevertheless, the approach could be useful in assessing the performance of a postharvest treatment in terms of reducing the damage progression over the storage period.

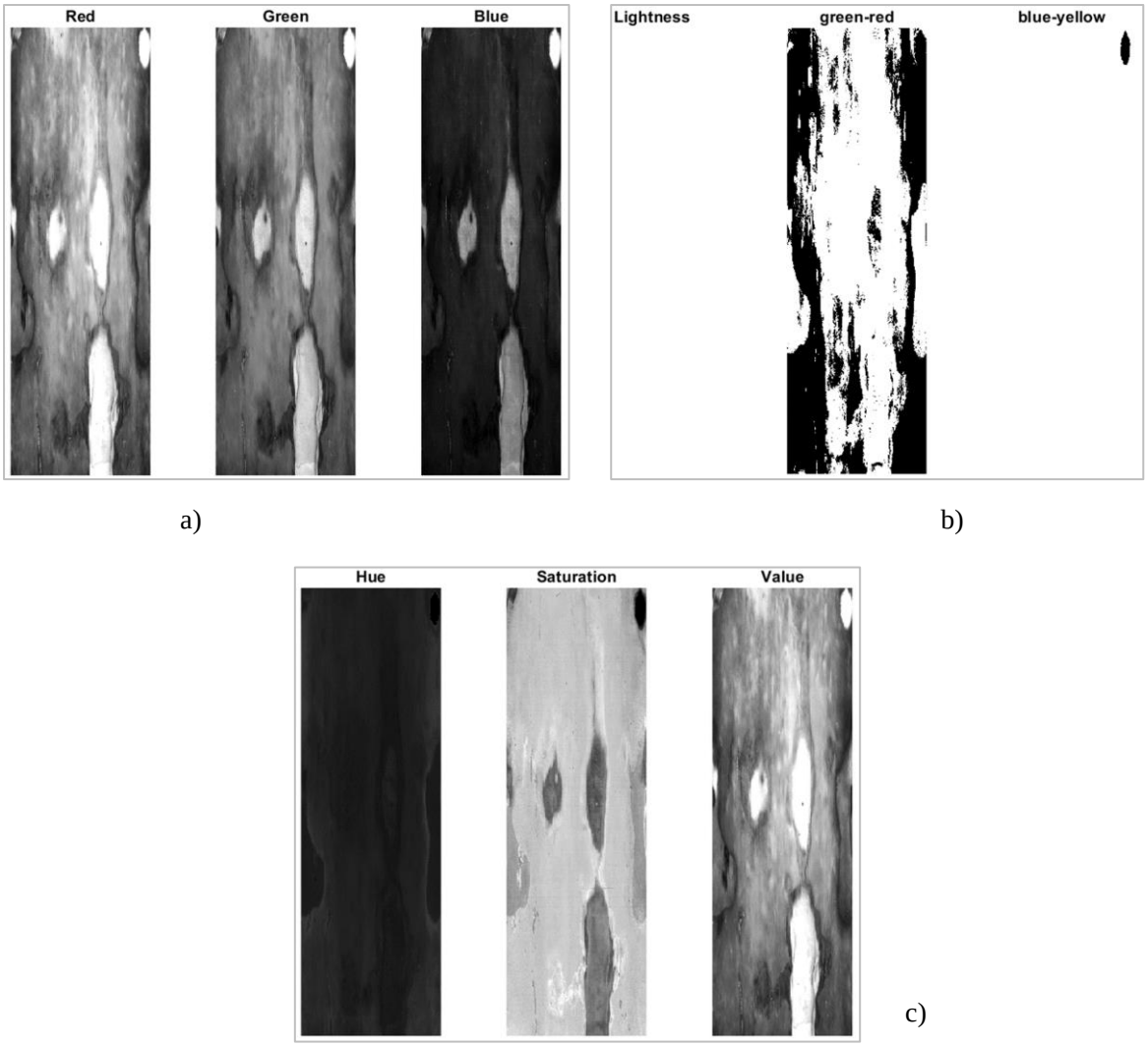

Figure 7. Visualization of images in the individual color channel for comparison

3.3 Identification of the Most Dominant Color Channels

The color space that was the most sensitive overall, i.e., could capture most of the information about the day-to-day color changes of cucumber was identified. To identify the most significant color component (R, G, B, L*, a*, b*, H, S, V) in a color space RGB, L*a*b*, and HSV, a principal component analysis (PCA) was carried out.

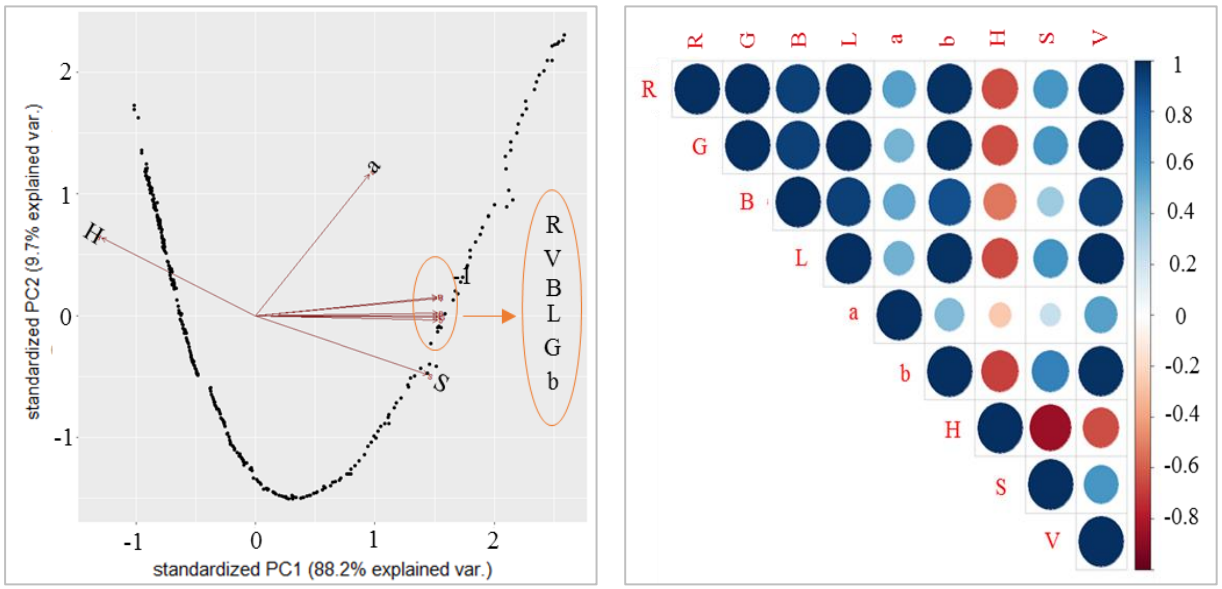

a) b)

Figure 8. A biplot of the first two components of a PCA model of the calibration data set (a) and correlation plot of the variables of the calibration data set (b)

Figure 8a shows a PCA biplot containing both PC scores (dots) and loading (arrows) of each variable on the axis. Therefore, the biplot visualizes the lines that account for the maximum variance and most significant information of the data. The plot also shows how the variables are correlated with each other; the variable H, which was placed on the other side of the plot, was negatively correlated with the other variables (Fig. 8a). From the correlation plot (Fig. 8b), it is clear that the variables R, G, B, L*, b*, and V were highly and positively correlated with each other. As it was already interpreted from the PCA biplot, there were negative correlations between H and the other components.

From Figure 8a, the explained variance by PC1 and PC2 is 88.2% and 9.7%, respectively. It is obvious that PC1 alone explained the majority of variance in the data set. It is imperative to know which variables contributed the most to PC1. A list of loadings that indicates the variables with high loadings on the first two principal components is shown in Table 2. From the loadings of the variables in Table 2, the variables that strongly contributed to PC1 were R, G, B, L*, b*, and V. On the other hand, the variables a*, H, and S contributed to PC2 and, therefore, did not contribute much to PC1. Hence, a*, H, and S can be designated as PC2. Also, from the biplot, the lines representing the variables R, G, B, L*, b*, and V were directed further from the PC origin. Therefore, these variables might capture the most variation in the data set. For further confirmation, a prediction about the principal components was made with two new independent data sets with the same variables. With the new validation data sets, PC1 still contained a majority of the information (75%) about the color changes by the same dominating variables as the calibration data (Fig. 9).

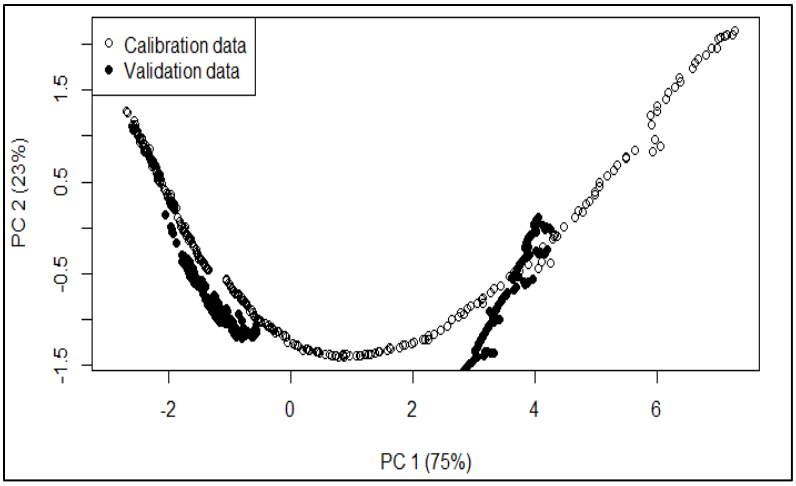

Figure 9. Prediction on the principal components with the new validation data sets

Table 2. Contributions (%) of variables to PC1 and PC2

Variables	Contributions			
	Calibration data		Validation data	
	PC1	PC2	PC1	PC2
R	0.35	0.11	0.36	0.00
G	0.35	0.01	0.36	0.07
B	0.35	0.01	0.36	0.09
L*	0.35	0.00	0.36	0.05
a*	0.22	0.81	0.13	0.96
b*	0.35	0.02	0.36	0.11
H	0.30	0.45	0.29	0.03
S	0.33	0.34	0.33	0.23
V	0.35	0.10	0.36	0.02

Table 2 shows that each R, G, and B component in the RGB color space performed as PC1. Unlike RGB, all three channels in L*a*b* and HSV did not contribute to PC1. For visualization, on the first day and last day (after two weeks) of imaging, RGB images and all three components in grayscale are shown in Fig. 10. The corresponding pixel value histograms are also shown. Figures 10 shows that all the individual R, G, and B components effectively represent the color changes of cucumbers from day 1 to day 14.

Similar to the present study, color changes during mango maturation were evaluated in CIELAB and HSV. However, using only a*, b*, S, and H coordinates offered adequate classification of ripeness after PCA analysis in selecting the most dominant variables (Vélez-Rivera et al., 2014). Group comparisons for papaya ripening achieved better predictions when normalized mean values of R, G, and B channels were used (Santos Pereira et al., 2018). The RGB color space is the fundamental color space that is transformed into other color spaces to better reflect human perception but the outcome is also devise-dependent (Vélez-Rivera et al., 2014). The RGB transformation to other colors can be done in two ways: linear and nonlinear. The transformations to HSV and *L*a*b** color spaces are examples of nonlinear transformation. Color spaces differ by characteristics, and their performance varies by the type of visual tasks (Yang et al., 2010; Bhargava & Bansal, 2021). In the present work, RGB color space was found to be suitable to get the necessary information about the external changes of cucumber. Therefore, no color transformation is required, and it is recommended to interpret the images as an RGB image.

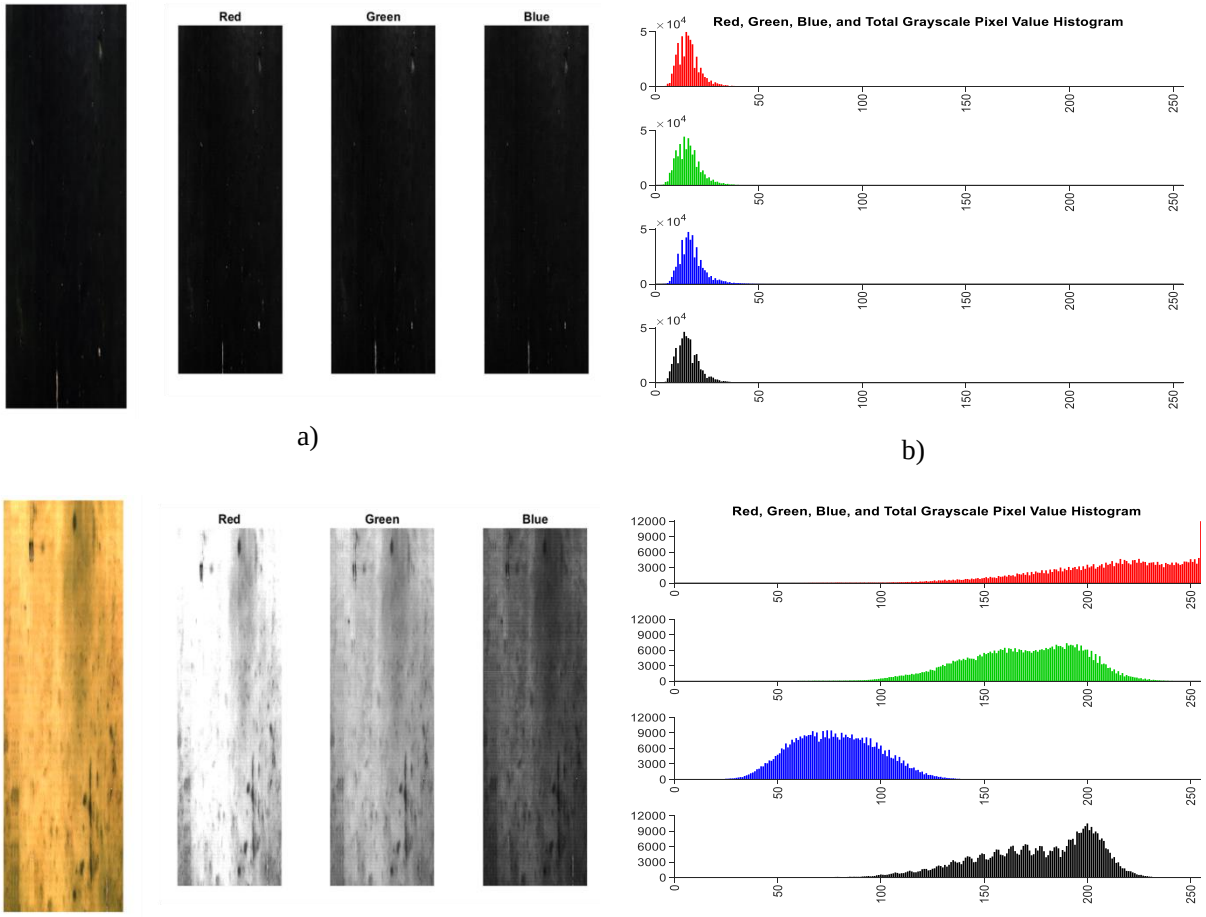

Figure 10. Visualization of Day 1 RGB image (a) with its corresponding grayscale red, green, and blue channel and pixel value histogram (b) and visualization of Day 14 RGB image (c) with its corresponding grayscale red, green, and blue channel and pixel value histogram (d)

4. Conclusions

In this study, a machine vision system was developed and utilized to monitor cucumbers' external quality during storage. External changes of stored cucumbers were evaluated by extracting color and creating Absolute Differential Damage Progression Plot. Comparing the grayscale histograms and the R, G, and B values over the storage period was found to be a suitable means of obtaining insight into the color changes of cucumber. Over time, in the color histogram plots, the pixel values of the image shifted from left to right, indicating the cucumber surface turning yellowish. Similarly, R, G, and B values had a steady increase as the color of the surface changed. The Blue (B) channel in RGB color space was found to be optimal for interpreting the damage progression from the absolute differential damage progression plot (ADDP) and the corresponding histogram. RGB images of the cucumbers were transformed into L*a*b* and HSV color spaces. The most sensitive color space, i.e., the space that could capture most of the information about the day-to-day color changes of cucumber, was identified by means of the Principal Component Analysis (PCA). According to the PCA on the test data, unlike L*a*b* and HSV color spaces, each of the individual channels in RGB space was found to be suitable to retain the necessary information about the external changes of cucumber. This observation was further validated with independent datasets. Overall, the machine vision approach could be a potential nondestructive technique for monitoring the external quality of cucumber as well as for evaluating the performance of any postharvest treatment during storage. In the future, the recognition or classification of the damage in a cucumber image should follow a standard procedure to be able to prevent it effectively.

Funding

This research received funding from Appropriate Scale Mechanization Consortium (ASMC). Open access was supported by USDA National Institute of Food and Agriculture Evans-Allen Capacity Grant to Dr. Ayesha Sarker.

Author Contribution

Ayesha Sarker: Conceptualization, experimentation, data analysis and original draft preparation. Tony Grift: Conceptualization, review and editing, and supervision.

Declaration of Conflicting Interests

None to declare.

Data Availability

Available from the corresponding author upon reasonable request.

References

Akundi, A., & Reyna, M. (2021). A Machine Vision Based Automated Quality Control System for Product Dimensional Analysis. *Procedia Computer Science, 185*, 127-134. https://doi.org/10.1016/j.procs.2021.05.014

Al-Rahbi, S., Manickavasagan, A., Al-Yahyai, R., Khriji, L., & Alahakoon, P. (2013). Detecting surface cracks on dates using color imaging technique. *Food Science and Technology Research, 19*(5), 795-804. https://doi.org/10.3136/fstr.19.795

Ariana, D. P., & Lu, R. (2010). Hyperspectral imaging for defect detection of pickling cucumbers. In D.-W. Sun (Ed.), *Hyperspectral imaging for food Quality analysis and control, First Edition* (pp. 431-447). Academic Press. https://doi.org/10.1016/B978-0-12-374753-2.10014-0

Bahnasawy, A. H., & Khater, E. G. (2014). Effect of wax coating on the quality of cucumber fruits during storage. *Food Processing & Technology, 5*(6), 1-8. https://doi.org/10.4172/2157-7110.1000339

Bhargava, A., & Bansal, A. (2021). Fruits and vegetables quality evaluation using computer vision: A review. *Journal of King Saud University - Computer and Information Sciences, 33*, 243-257. https://doi.org/10.1016/j.jksuci.2018.06.002

Chherawala, Y., Lepage, R., & Doyon, G. (2006). Food grading/sorting based on color appearance trough machine vision: the case of fresh cranberries. *2nd International Conference on Information & Communication Technologies*, 1540-1545. https://doi.org/10.1109/ICTTA.2006.1684612

Cubero, S., Aleixos, N., Moltó, E., Gómez-Sanchis, J., & Blasco, J. (2011). Advances in machine vision applications for automatic inspection and quality evaluation of fruits and vegetables. *Food and Bioprocess Technology, 4*, 487-504. https://doi.org/10.1007/s11947-010-0411-8

Du, C. J., & Sun, D. W. (2006). Learning techniques used in computer vision for food quality evaluation: A review. *Journal of Food Engineering, 72*(1), 39-55. https://doi.org/10.1016/j.jfoodeng.2004.11.017

Fathi, M., Mohebbi, M., & Razavi, S. M. A. (2009). Application of image analysis and artificial neural network to predict mass transfer kinetics and color changes of osmotically dehydrated kiwifruit. *Food and Bioprocess Technology, 4*(8), 1357-1366. https://doi.org/10.1007/s11947-009-0222-y

Gardner, J. L. (2007). Comparison of calibration methods for for tristimulus colorimeters. *Journal of Research of the National Institute of Standards and Technology, 112*(3), 129-138. https://doi.org/10.6028/jres.112.010

Grift, T. E., Novais, J., & Bohn, M. (2011). High-throughput phenotyping technology for maize roots. *Biosystems Engineering, 110*(1), 40-48. https://doi.org/10.1016/j.biosystemseng.2011.06.004

Grift, T. E., Zhao, W., Momin, M. A., Zhang, Y., & Bohn, M. O. (2017). Semi-automated, machine vision based maize kernel counting on the ear. *Biosystems Engineering, 164*, 171-180. https://doi.org/10.1016/j.biosystemseng.2017.10.010

Iqbal, S. M., Gopal, A., Sankaranarayanan, P. E., & Nair, A. B. (2016). Classification of Selected Citrus Fruits Based on Color Using Machine Vision System. *International Journal of Food Properties, 19*(2), 272-288. https://doi.org/10.1080/10942912.2015.1020439

Kang, S. P., East, A. R., & Trujillo, F. J. (2008). Colour vision system evaluation of bicolour fruit: A case study with "B74" mango. *Postharvest Biology and Technology, 49*(1), 77-85.

https://doi.org/10.1016/j.postharvbio.2007.12.011

Kondo, N. (2010). Automation on fruit and vegetable grading system and food traceability. *Trends in Food Science and Technology, 21*(3), 145-152. https://doi.org/10.1016/j.tifs.2009.09.002

Maleki, G., Sedaghat, N., Woltering, E. J., Farhoodi, M., & Mohebbi, M. (2018). Chitosan-limonene coating in combination with modified atmosphere packaging preserve postharvest quality of cucumber during storage. *Journal of Food Measurement and Characterization, 12*(3), 1610-1621. https://doi.org/10.1007/s11694-018-9776-6

Mendoza, F., Dejmek, P., & Aguilera, J. M. (2006). Calibrated color measurements of agricultural foods using image analysis. *Postharvest Biology and Technology, 41*, 285-295. https://doi.org/10.1016/j.postharvbio.2006.04.004

Mohammadi, A., Hashemi, M., & Hosseini, S. M. (2016). Postharvest treatment of nanochitosan-based coating loaded with Zataria multiflora essential oil improves antioxidant activity and extends shelf-life of cucumber. *Innovative Food Science and Emerging Technologies, 33,* 580-588. https://doi.org/10.1016/j.ifset.2015.10.015

Mohammadi, V., Kheiralipour, K., & Ghasemi-Varnamkhasti, M. (2015). Detecting maturity of persimmon fruit based on image processing technique. *Scientia Horticulturae, 184*, 123-128. https://doi.org/10.1016/j.scienta.2014.12.037

Momin, A., Yamamoto, K., Miyamoto, M., Kondo, N., & Grift, T. (2017). Machine vision based soybean quality evaluation. *Computers and Electronics in Agriculture, 140*, 452-460. https://doi.org/10.1016/j.compag.2017.06.023

New Guyana Marketing Corporation. (n.d.). *Cucumbers: postharvest care and market preparation information sheet*. New Guyana Marketing Corporation (NGMC). Retrieved from http://www.newgmc.com/gmc_docs/brochures/Cucumber.pdf

Nicolaï, B. M., Defraeye, T., De Ketelaere, B., Herremans, E., Hertog, M. L. A. T. M., … Saeys, W. (2014). Nondestructive measurement of fruit and vegetable quality. *Annual Review of Food Science and Technology, 5*(1), 285-312. https://doi.org/10.1146/annurev-food-030713-092410

R Core Team. (2019). *R: A language and environment for statistical computing. R Foundation for Statistical Computing. Vienna, Austria*.

Santos Pereira, L. F., Barbon Jr., S., Valous, N. A., & Barbin, D. F. (2018). Predicting the ripening of papaya fruit with digital imaging and random forests. *Computers and Electronics in Agriculture, 145*, 76-82. https://doi.org/10.1016/j.compag.2017.12.029

Sarker, A., Deltsidis, A., & Grift, T. E. (2021). Effect of Aloe vera gel-Carboxymethyl Cellulose composite coating on the degradation kinetics of cucumber. *Journal of Biosystems Engineering, 46,* 112-128. https://doi.org/10.1007/s42853-021-00092-z

Vélez-Rivera, N., Blasco, J., Chanona-Pérez, J., Calderón-Domínguez, G., de Jesús Perea-Flores, M., … Arzate-Vázquez, I. (2014). Computer Vision System Applied to Classification of "Manila" Mangoes During Ripening Process. *Food and Bioprocess Technology, 7*(4), 1183-1194. https://doi.org/10.1007/s11947-013-1142-4

Yang, J., Liu, C., & Zhang, L. (2010). Color space normalization: Enhancing the discriminating power of color spaces for face recognition. *Pattern Recognition, 43*(4), 1454-1466. https://doi.org/10.1016/j.patcog.2009.11.014